Food and Chemical Toxicology 48 (2010) 2872–2880

Contents lists available at ScienceDirect

Food and Chemical Toxicology

journal homepage: www.elsevier.com/locate/foodchemtox

Aqueous extract of ginger shows antiproliferative activity through disruption of microtubule network of cancer cells

Diptiman Choudhury, Amlan Das, Abhijit Bhattacharya, Gopal Chakrabarti *

Department of Biotechnology and Dr. B.C. Guha Centre for Genetic Engineering and Biotechnology, University of Calcutta, 35 Ballygunge Circular Road, Kolkata, WB 700 019, India

ARTICLE INFO

Article history:
Received 21 January 2010
Accepted 15 July 2010

Keywords:
Natural poly-phenols
Anti-cancer activity
Apoptosis and cell signaling
Microtubule disruption
Tubulin binding new anti-cancer agent

ABSTRACT

Ginger has a long history of use as traditional medicine for varied human disease. Our present study has shown that the aqueous extract of ginger (GAE) interacts directly with cellular microtubules and disrupts its structure and induces apoptosis of cancer cells as well. The IC_{50} values of GAE, as determined from cell viability experiment on human non-small lung epithelium cancer (A549) cells and human cervical epithelial carcinoma (HeLa), were 239.4 + 7.4 and 253.4 + 8.9 μg/ml, respectively. It has been found that the apoptosis of A549 cells by GAE is mediated by up regulation of tumor suppressor gene p53 and alteration of the normal Bax/Bcl-2 ratio followed by down regulation of cellular pro-caspase3. The morphological change of cells upon GAE treatment has also been demonstrated. Both the structural and functional properties of tubulin and microtubule were lost, as confirmed by both ex vivo and *in vitro* experiments. The major component of GAE is poly-phenols (around 2.5%), which consist of ~80% flavones and flavonols. Poly-phenolic compounds are well known to have anti-mitotic properties, and may be further screened for the development of a potential anti-cancer agent.

1. Introduction

Ginger (*Zingiber officinale*) is a plant from *Zingiberaceae* family. Ginger (underground stem known as *rhizome*) has been used as a spice in south Asian countries including India and China for many years. Ginger as a traditional medicine has been used to treat pregnancy, vomiting, motion sickness, arthritis, cough and cold. It has also been used as an antioxidant, antimicrobial, and antifungal agent since long time (White, 2007). Ginger is rich in both hydrophilic and hydrophobic constituents. Among the small molecules, the hydrophobic portion of ginger extract contains mainly different kinds of monoterpens, oxygenated monoterpens, sesquiterpenes, zingerone, paradols, gingerols and shogaols other than essential oils (Saha et al., 2003). The hydrophilic portion of ginger extract mostly has different kinds of poly-phenolic compounds (Kato et al., 2006).

Different dietary factors are the source of many useful compounds for anti-cancer treatment (Khan et al., 2007). It has been reported that 6-gingerol (Lee et al., 2007) is a constituent of hydrophobic portion of ginger extract and has anti-cancer properties. The mechanism of action of this compound is not yet well studied. It has been reported that the chloroform extract of another species of *Zingiber* (*Zingiber cassumunar*) showed cell cycle arrest at G_0/G_1 phase of cell cycle of A549 cells. Though the presence of huge amount of poly-phenolic compounds in aqueous ginger extract has been reported, any report regarding the anti-cancer activity has not been reported yet. Therefore, we were interested to investigate the anti-cancer activity of GAE poly-phenols.

In this study, we examined the effects of aqueous extract of ginger on tubulin and microtubule, one of the important targets for cancer therapy. Microtubules are composed of polymer of tubulin heterodimers, a major cytoskeleton protein. It is highly dynamic in nature and has versatile functions in cells. Microtubule is involved in a number of important cellular functions such as segregation of the chromosomes during mitosis and meiosis and maintenance of the cellular cytoskeleton structure (Lodish et al., 2000). Normal cell division requires proper construction of the mitotic spindle apparatus, and microtubule dynamics play a critical role during the formation and in function of this spindle apparatus. The tubulin and microtubule equilibrium in a cell has been one of the most successful targets for anti-cancer drug development; such drugs bind either tubulin or the microtubule and affect the dynamicity of microtubules (Downing, 2000; Jordan and Wilson, 2004; Acharya et al., 2008, 2009; Panda et al., 1998; Lopus and Panda,

Abbreviations: GAE, ginger aqueous extract; PIPES, 1,4-piperazinediethanesulfonic acid; EGTA, ethylene bis (oxyethylenenitrilo) tetraacetic acid; BrdU, 5-bromo-2-deoxyuridine; GTP, guanosine 5′-triphosphate; DAPI, 4′,6-diamidino-2-phenylindole; PI, propidiumiodide; FITC, fluoresceinisothiocyanate; MTT, (3-(4,5-dimethylthiazolyl-2)-2,5-diphenyltetrazoliumbromide); kDa, kilo Dalton; IC_{50}, 50% inhibitory dose; GA_{eq}, gallic acid equivalent.

* Corresponding author. Tel.: +91 33 2461 5445; fax: +91 33 2461 4849.
E-mail address: gcbcg@caluniv.ac.in (G. Chakrabarti).

0278-6915/$ - see front matter © 2010 Elsevier Ltd. All rights reserved.
doi:10.1016/j.fct.2010.07.020

2006; Leoni et al., 2000). Many of such molecules have been isolated from natural sources and used in cancer therapy for many years; e.g. paclitaxel, isolated from *Taxus brevifolia*, is used for treatment of various types of cancers; vincristine, purified from *Catharanthus coseus*, is used for the treatment of acute lymoblastic lymphoma (ALL).

In this work, we demonstrated that aqueous extract of ginger (GAE) directly disrupts microtubule networks in cells that leads to apoptosis of A549 cells via mitochondrial death cascade. According to the result of *in vitro* studies, GAE binds tubulin and inhibits tubulin polymerization. Thus, GAE could be evaluated for its clinical use against cancers.

2. Materials and methods

2.1. Materials

Nutrient Ham's F12 (supplemented with 1 mM L-glutamine), Bovine Fetal Serum, penicillin–streptomycin mixture and 100 mM fungizone were purchased from HyClone, USA. Trypsin-Versene was purchased from Cambrex Bioscience, USA. BrdU cell proliferation assay kit, Calbiochem, USA. DAPI, FITC-conjugated monoclonal anti-α-tubulin antibody (raised in mouse), mouse monoclonal anti-p53 antibody, mouse monoclonal anti-Bcl-2, mouse monoclonal anti-Bax antibody, mouse monoclonal anti-α-tubulin antibody (without conjugation), goat monoclonal rhodamine-conjugated IgG antibody, GTP PIPES, EGTA, RNase A, and propidium iodide (PI) were purchased from SIGMA, USA. Goat monoclonal anti-mouse HRP-conjugated secondary antibody and Bradford Protein estimation kit were purchased from GeNei, India. Annexin V-FITC apoptosis detection kit was obtained from BD Biosciences, San Diego, CA, USA. Folin–Ciocalteu reagent and other chemicals are analytical grade and were purchased from Sisco Research Laboratories, India.

2.2. Preparation of ginger aqueous extract

Fresh ginger tissues (tuber) were collected form Himalayan Dooars region and homogenized in water and the supernatant was taken after centrifugation at 100,000*g* for 1 h and evaporated to dryness at 60 °C. The dried pellet was then extracted at 60 °C in hot petroleum ether (PET) boiling temperature 60–80 °C. After several repetitive (10 cycles) extraction cycles with PET, the dried tissue mass was subsequently subjected to 10 repetitive cycles of hot chloroform extraction (56 °C). After removal of all hydrophobic parts form the tissue mass, it was subjected to 10 repetitive cycles of hot water (60 °C) extraction. This supernatant was then extracted with 100% cold methanol for removal of residual portion of proteins. After removal of proteins from the extract, the supernatant was lyophilized. We obtained 2.5 g of dried extract from 2 kg of fresh ginger tissue. For final use it was dissolved in water or in the required buffer and termed as ginger aqueous extract (GAE). The 5 mg/ml stock was used for experimental purposes.

2.3. Estimation of total phenol content in GAE

Total phenolic content in GAE was estimated by Folin–Ciocalteu assay (Singleton et al., 1999). For phenolic compounds estimation, different concentrations (1, 2 and 5 mg/ml) of stock GAE extract were prepared. 50 μl of Folin–Ciocalteu reagent were added to 250 μl of the extract and kept for 6 min at room temperature in dark. After the incubation, 500 μl of 7% sodium carbonate solution was added and kept for 60 min. Then the volume was adjusted to 1.3 ml by adding distilled water. Absorbances were measured at 765 nm. To prepare standard curve of gallic acid, 2–40 μg/ml of gallic acid was used. The results were expressed as gallic acid equivalent (GA_{eq})/mg of GAE (Singleton et al., 1999).

2.4. Estimation of total flavones and flavonol content in GAE

The contents of flavones and flavonols in GAE are expressed as quercetin equivalent (Q_{eu}). For making the calibration curve, standard solutions (5.0–50.0) μg/ml in 80% ethanol (v/v) of quercetin were used. The GAE solutions 5 mg/ml (0.5 mL) were mixed with 1.5 ml 95% ethanol (v/v), 0.1 mL 10% aluminum chloride (m/V), 0.1 mL of 1 mol L^{-1} potassium acetate and 2.8 ml water. The volume of 10% (m/V) aluminum chloride was substituted by the same volume of distilled water in blank. After incubation at room temperature for 30 min, the absorbance of the reaction mixture was measured at 415 nm (Wu et al., 2009).

2.5. Purification of tubulin

Tubulin was isolated from goat brain by two cycles of temperature-dependent polymerization and depolymerization in PEM buffer (50 mM PIPES, pH 6.9; 1 mM EGTA, and 1 mM $MgCl_2$) and 1 mM GTP followed by two more cycles of polymerization and depolymerization in GEM buffer (1 M sodium glutamate, pH 6.9; 1 mM EGTA, and 1 mM $MgCl_2$) (Hamel and Lin, 1981). The protein concentration was estimated by the method of Bradford (Bradford, 1976) using bovine serum albumin as the standard. Aliquots were flash frozen in liquid nitrogen and stored at −70 °C.

2.6. Human cells culture and counting

Human cervical carcinoma (HeLa) cells were maintained in DMEM nutrient medium supplemented with 1 mM L-glutamine, 10% fetal bovine serum, 0.37% $NaHCO_3$ 1 mM penicillin, 1 mM streptomycin and 1 mM fungizone (pH 7.4). Human lung carcinoma (A549) cells were maintained in Ham's F12 supplemented with 1 mM L-glutamine, 10% fetal bovine serum, 0.2% $NaHCO_3$ 1 mM penicillin, 1 mM streptomycin and 1 mM fungizone (pH 7.4). The cells were cultured at 37 °C in a humidified atmosphere containing 5% CO_2.

2.7. Cell viability assay

Cell viability was assessed by trypan blue dye exclusion method and MTT assay. For trypan blue assay, cultured cells (1×10^6 cells per well) were plated in each 35 mm petridish and GAE doses were added in increasing order. After 24 h of incubation, cell counting was done as previously described.

For MTT assay, both A549 and HeLa cells were seeded in 96-well plates at 1×10^4 cells per well and were allowed to grow to 70–80% confluency and the cells were treated with different concentrations of GAE for 24 h. Treated cells were incubated with MTT (2 mg/ml in 5% ethanol) for 6 h at 37 °C, the medium was removed and dye crystal formazan was solubilized in 200 μl dimethyl sulphoxide (DMSO). The absorbance was measured at 570 nm. Data were calculated as the percentage of inhibition according to the following formula:

$$\% \text{ inhibition} = [100 - (A_t/A_s) \times 100] \times \%. \quad (1)$$

A_t and A_s are the absorbances of the test substances and solvent control, respectively (Acharya et al., 2009).

2.8. Effect of GAE on cellular DNA synthesis

Cultured A549 cells were treated with different concentrations of GAE for 24 h. To demonstrate the utility of 5-bromo-2-deoxyuridine (BrdU) 20 μl of 5′ BrdU in (1:2000 dilutions) was added to the medium immediately after the addition of GAE. After completion of the incubation, samples were processed according to BrdU cell proliferation assay kit protocol of Calbiochem and absorbance was measured by an ELISA reader at dual wavelengths 450 and 540 nm.

2.9. Effect of GAE on cell cycle progression

Cultured HeLa and A549 cells were treated with different doses of GAE for 24 h. The cells were fixed using chilled 100% methanol and incubated with 100 μl of RNase solution (500 unit/ml) at 37 °C for 3 h. Then the nuclear DNA was labeled with propidium iodide (PI) (0.05 mg/ml). Cell cycle phase distribution of nuclear DNA was determined on FACScalibur having fluorescence detector equipped with 488 nm argon laser light source and 623 nm band pass filter (linear scale), and data were analyzed using Cell Quest software (Becton Dickinson). A total of 10,000 events were acquired.

2.10. Flow cytometric analysis for apoptotic cells

To examine the induction of apoptosis by GAE, cultured A549 cells (1×10^6) were treated with different concentrations of GAE for 24 h. The cells were then stained for 30 min at room temperature in the dark with fluorescein isothiocyanate (FITC)-conjugated Annexin V (1 μg/ml) and PI (50 μg/ml) in a Ca^{2+}-enriched binding buffer and analyzed by a two-color flow cytometric assay using a FACSCalibur flow cytometer as described in Acharya et al. (2009). For each set a total of 10,000 event counts were taken. Again, after being stained, images were taken with Zeiss LSM 510 Meta Confocal microscope (the fluorochrome was excited at 488 nm and images were taken with 63× oil immersion lens) and the images were processed with LSM software.

2.11. JC-1 stain of GAE-treated A549 cells for monitoring of change of mitochondrial membrane potential

Cultured A549 cells (1×10^6) were treated with different doses of GAE for 24 h. The cells were harvested in 50 μl PBS and incubated with JC-1 (5,5′,6,6′-tetrachloro-1,1′,3,3′-tetraethylbenzimidazol-carbocyanine iodide) at 5 μg/ml for 10 min at room temperature, and the final volume was adjusted to 500 μl. The samples were analysed by flowcytometer (Xin-Yi et al., 2008).

2.12. Western blot analysis of GAE-treated A549 cells

Untreated (control) and GAE (250 μg/ml)-treated A549 cells were used for western blot analysis. Fifty micrograms of whole cell extract (after lysis in hypotonic lyses buffer) were loaded onto gel in each lane. Western blot analysis to observe cellular p53 level was done using mouse monoclonal IgG anti-p53 antibody (1:7500 dilutions). For the detection of anti-apoptotic Bcl-2 level and pro-apoptotic Bax proteins mouse monoclonal IgG primary antibody (1:1000 dilutions) and HRP-conjugated anti mice IgG secondary antibody were used (1:2000 dilutions). For the detection of cellular pro-caspase3 status, goat monoclonal IgG was used at a dilution of 1:1000 and the corresponding secondary antibody was used (1:2500 dilution).

2.13. Effect of GAE on cellular morphology and interphase microtubule of A549 and HeLa cells

Cultured A549 and HeLa cells were grown on sterile cover slips at a density of 1×10^6 cells/ml and incubated with different doses of GAE for 24 h. Bright field images of cells were taken by Olympus inverted microscope model CKX41. Then the cells were processed for confocal microscopic study (Acharya et al., 2009). Tubulin of A549 cells was stained with mouse monoclonal FITC-conjugated anti-α-tubulin antibody- (1:50 dilution), and tubulin of HeLa cells was stained with mouse monoclonal anti-α-tubulin primary IgG antibody (at 1:200 dilution) and rhodamine-conjugated goat monoclonal anti-mouse IgG secondary antibody (1:100). DAPI was used to stain the cell nucleus (1:500 dilution of 1 mg/ml stock solution). Images were taken with Zeiss LSM 510 Meta Confocal microscope (at 488 nm with 63× oil immersion lens), and the images were processed with LSM software (Acharya et al., 2009; Das et al., 2009).

2.14. Reassembly of microtubules in presence of GAE after cold depolymerization microtubules of A549 cells

A549 and HeLa cells (1×10^6 cells/ml) were grown on glass cover slips for 24 h and then incubated at 4 °C for 5 h. After cold treatment, the cold medium was replaced with warm medium containing different doses of GAE and incubated at 37 °C. The cells were then fixed after 2 h with 2% (v/v) p-formaldehyde at room temperature for 1 h incubation. The cells were processed in the same way as before. Microtubules were observed using a Ziess LSM 510 Meta confocal microscope (Acharya et al., 2009).

2.15. Inhibition of tubulin polymerization by GAE in vitro

Purified mammalian tubulin (10 μM) was mixed with different concentrations of GAE, and polymerization reaction was initiated in GEM buffer at 37 °C just after adding 1 mM GTP in the assembly mixture. The rate and extent of the polymerization reaction were monitored by the extent of light scattering at 350 nm for 15 min using V-630 Jasco Spectrophotometer equipped with a variable temperature water bath (Gaskin et al., 1974). For each dose five mutually independent observations were taken.

3. Results

3.1. Estimation of total phenolic contents and flavones, flavonols contents of GAE

The total phenolic contents in GAE were measured by Folin–Ciocalteu assay (Singleton et al., 1999) using gallic acid (GA) as the standard. The amount of phenolic compounds in GAE is 25 μg/mg GA_{eq}. The total flavones–flavanols contents in GAE were estimated by colorimetric assay using quercetin (Q) as the standard. Total flavones–flavonols present in GAE is 20.1 μg/mg Q_{eq}.

3.2. GAE causes loss of cell viability

Ginger aqueous extract (GAE) contains good amount of polyphenols and flavones–flavanols. As natural poly-phenols and flavones–flavonols show anti-cancer activity, we would like to examine the effect of GAE on cell viability of cancer cells by MTT assay and trypan blue exclusion assay. Cultured A549 cells were incubated in the absence and the presence of 10–500 μg/ml of GAE for 24 h. MTT assay was performed for the determination of cell viability (details in Section 2). Ginger aqueous extract (GAE) caused loss of cell viability of A549 cells in a concentration-dependent manner (Fig. 1A). At lower concentrations, no significant loss of cell viability was observed. For example, at 10 and 25 μg/ml of GAE, loss of cell viability was 0.5% and 4.5%, respectively. Whereas at 50, 125 and 250 μg/ml, loss of cell viability was 10.5%, 23.4% and 53.4%, respectively. The calculated IC_{50} value for GAE for A549 cells is 239.4 + 7.4 μg/ml. For HeLa cells, the IC_{50} value for GAE is 253.4 + 1.9 μg/ml as determined by MTT assay (Fig. 1B). Determination of cell viability of A549 cells and HeLa cells in the presence of GAE by trypan blue assay (described in the Section 2) showed similar results like MTT assay. Fig. 1C represents plots of percent-

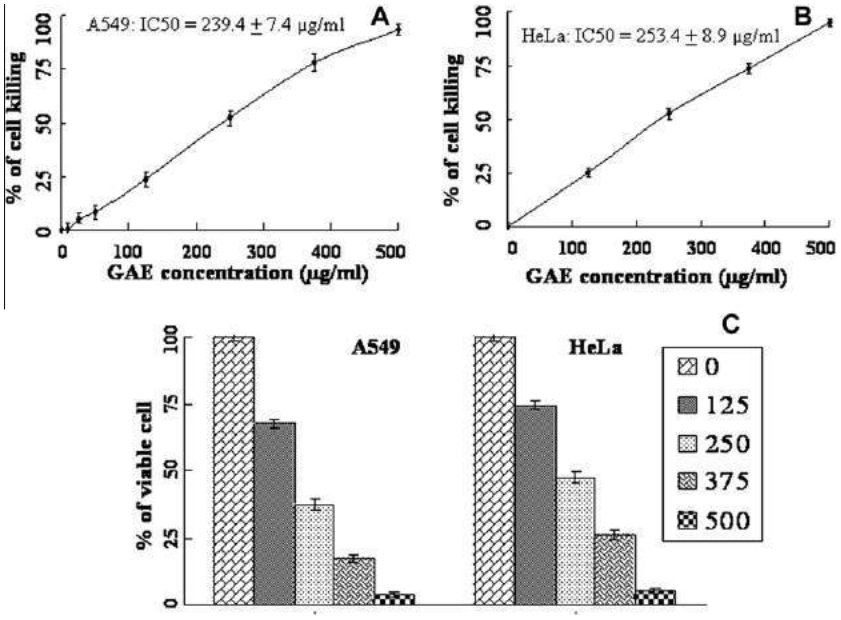

Fig. 1. Cell viability assays for cancer cells after treatment with GAE. (A) MTT assay for A549 cells. Results of the MTT assay for A549 cells treated with 0, 10, 25, 50, 125, 250, 375 and 500 μg/ml of GAE for 24 h. (B) MTT assay for HeLa cells. Results of the MTT assay of HeLa cells treated with 0, 125, 250, 375 and 500 μg/ml of GAE for 24 h. Data represent mean ± SD of five independent experiments. (C) Trypan blue assay for A549 and HeLa cells. Results of trypan blue assay with A549 and HeLa cells treated with (0–500 μg/ml) GAE for 24 h. Details of the MTT assay and trypan blue assay are described in Section 2.

age of viable cells against concentration of GAE. The IC_{50} values for GAE for both A549 and HeLa cells are similar to those of MTT assay.

3.3. Effect of GAE on cell cycle progression

Cell cycle progression of A549 and HeLa cells in the presence GAE was monitored by flow cytometer. Cultured A549 cells were incubated with various doses of GAE (10–250 μg/ml) for 24 h, and cell cycle analysis was performed using FAScan flow cytometer and the results are presented in Fig. 2. The population of cells in subG_0/G_1 phase was increased in a dose-dependent manner. At lower concentrations of GAE (10–50 μg/ml), no significant amount of population of cells were in subG_0/G_1 phase. At doses of 10, 25 and 50 μg/ml of GAE, only 3.92%, 7.05% and 11.6%, respectively, population of cells were in subG_0/G_1 phase (Fig. 2). In case control sample (untreated), 2.18% cells were in subG_0/G_1 phase. However, 30.15% and 59.02% cells were found to be in subG_0/G_1 phase, when A549 cells were treated with 125 and 250 μg/ml GAE, respectively (Fig. 2). As lower concentration of GAE did not have significant effect on cell cycle progression of A549 cells; therefore, in the case of HeLa cells, we kept the higher concentration GAE and performed the cell cycle assay. For HeLa cells, 23.33% and 53.40% cells were found to be in subG_0/G_1 phase, when treated with 125 and 250 μg/ml of GAE for 24 h, respectively, whereas only 4.98% cells were in the subG_0/G_1 phase in the case of control (untreated) HeLa cells (Fig. 2).

3.4. Confirmation of apoptosis in GAE-treated A549 cells

Apoptosis of A549 cells was monitored using FITC–annexin-V and propidium iodide (PI) double staining by FACS, after treatment of cells with (0–250 μg/ml) of GAE for 24 h. As shown in Fig. 3, GAE induces apoptosis in A549 cells. The amounts of early apoptotic cells (annexin-V positive and PI negative) were 0.08%, 0.15%, 0.42%, 2.36%, 4.86% and 18.36% for 0, 25, 50, 125 and 250 μg/ml, respectively, and the amounts of late apoptotic cells (annexin-V positive and PI positive) were 0.83%, 1.47%, 4.46%, 10.51%, 20.5% and 29.74% for the same doses, respectively. At lower doses (10 and 25 μg/ml), the amounts of early and late apoptotic populations were less significant but upon increment of dose the amount of apoptotic population had increased dramatically.

3.5. Changes in the mitochondrial membrane potential of A549 cells by GAE

As GAE induced apoptosis in A549 cells and caused cell death, we were interested to examine the effect of GAE on mitochondrial membrane potential (MMP) of A549 cells. Changes in the mitochondrial membrane potential of A549 cells were monitored with the fluorescent probe JC-1 by FACS. Flow cytometry analysis of GAE-treated A549 cells demonstrated a decrease in the population having red fluorescence (FL-2) accompanied by a slight increase in the population green fluorescence (FL-1) (Fig. 4A). The median values of FL-2 fluorescence were decreased from 421.7 ± 10 (untreated control) to 278.81 ± 12 and 164.00 ± 8 in the presence of 125 and 250 μg/ml GAE, respectively, and the FL-1 fluorescence was increased from 139.49 ± 10 (of control) to 148.5 ± 12 and 210 ± 11 in the presence of similar doses of GAE, respectively. These results indicated that treatment of GAE to A549 cells causes reduction of mitochondrial membrane potential.

3.6. Western blot analysis for detection of cellular protein expression level in GAE-treated A549 cells

As we confirmed the cellular apoptosis of A549 cells and HeLa cells by GAE and found the change of mitochondrial membrane potential of A549 cells by GAE, we were interested to see the expression level of different pro- and anti-apoptotic proteins. Cultured

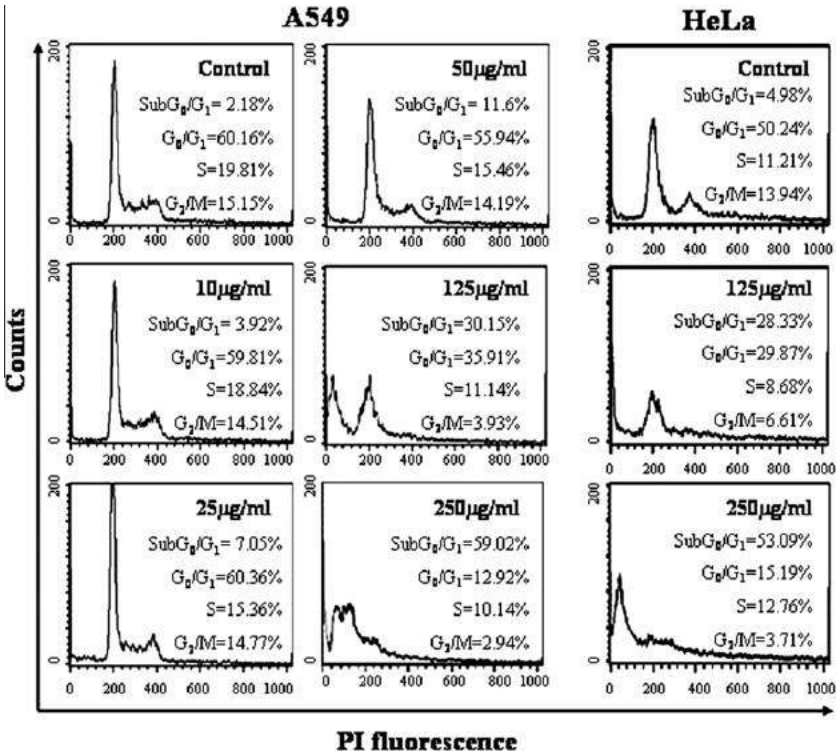

Fig. 2. Flow cytometric analysis of the cell cycle distribution of GAE-treated A549 and HeLa cells. Cultured A549 cells were treated with 0, 10, 25, 50, 125 and 250 μg/ml of GAE for 24 h and HeLa cells were treated with 0, 125 and 250 μg/ml of GAE for 24 h. Cell cycle analysis was performed using BD FACScalibur. Details of the experiment are given in Section 2.

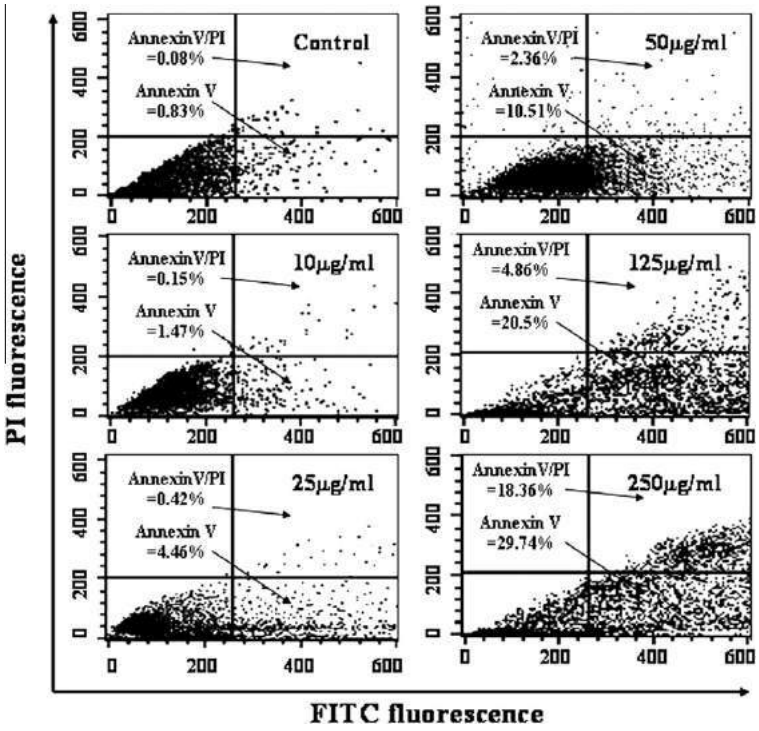

Fig. 3. Determination of apoptosis of GAE-treated A549 cells. Cultured A549 cells were treated with (0–250) μg/ml GAE, and apoptosis was monitored by annexin-V-FITC and PI double staining. Apoptotic cells were analyzed by flow cytometer, and a dot plot representation of annexin-V-FITC fluorescence (*X*-axis) vs. PI fluorescence (*Y*-axis) has been presented. The percentage of early apoptotic cells (annexin-V-positive and PI negative cells) located in the bottom right quadrant as well as late apoptotic cells (annexin-V and PI double positive cells) located in the top right quadrant is shown.

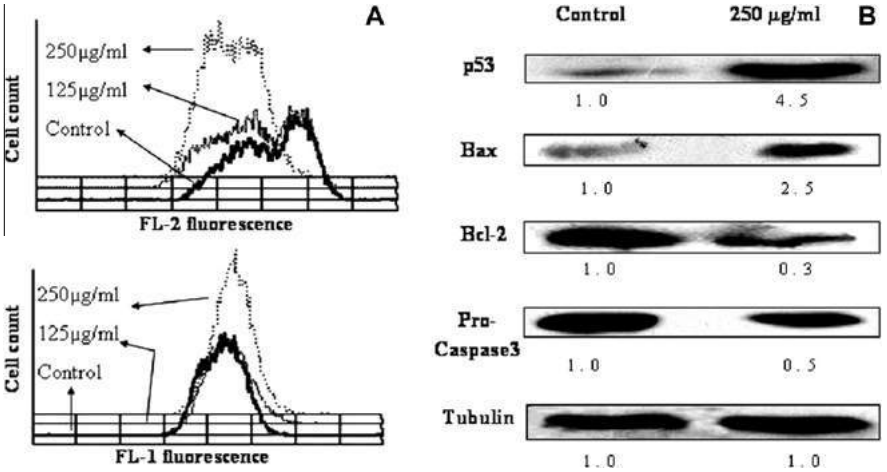

Fig. 4. Loss of mitochondrial membrane potential and modulation of the pro- and anti-apoptotic proteins in GAE-treated cells. (A) Reduction of mitochondrial membrane potential in GAE-treated A549 cells. Cultured A549 cells were treated with (0–250) μg/ml of GAE for 24 h, stained with JC-1, and analyzed by flow cytometer. Shift of fluorescence of FL-2 (upper) and FL-1 (lower) of GAE-treated A549 cells. Green fluorescence and red fluorescence were detected by FL-1 and FL-2 filters, respectively, details of the experiment are given in Section 2. (B) Western blot analysis of GAE-treated A549 cells for determination of expression level of cell cycle regulatory proteins. Cultured A549 cells treated with 0 and 250 μg/ml of GAE and status of pro- and anti-apoptotic proteins were monitored by Western blot analysis using mouse monoclonal anti-p53, anti-Bax, anti-Bcl-2, and anti-pro-caspase3 antibodies. Mouse monoclonal anti-α-tubulin antibody was used for loading controls. The relative band intensity is mentioned under each figure.

A549 cells showed very low level of p53 expression, and GAE treatment resulted in 4.5-fold increment of p53 expression in A549 cells after treatment with a 250 μg/ml GAE (Fig. 4B). We were then interested to check the status of cellular Bax/Bcl-2 ratio. We found up regulation of pro-apoptotic protein Bax (by 2.5-fold) and down regulation of anti-apoptotic protein Bcl-2 (by 0.3-fold) at a 250 μg/ml dose of GAE in A549 cells (Fig. 4B). Hence the Bax/Bcl-2 ratio is increased. Increment of Bax/Bcl-2 ratio usually leads cells to apoptosis via caspase-dependent pathway. In this pathway, the ultimate mediator of cellular apoptosis is caspase3. Usually in cells caspase3 expresses as a pro-caspase3, which is a 32 kDa protein. When cells go through apoptosis via caspase-dependent pathway, pro-caspase3 goes to proteolytic cleavage giving rise to active caspase3 (17–19 KD), leading to cellular apoptosis. Hence, the decrease in pro-caspase3 in treated cells shows an increase of active caspase3. At 24 h of GAE treatment, we found a decrease in pro-caspase3 level (by 0.5-fold) when compared with the untreated A549 cells (Fig. 4B). Western blotting of total cellular tubu-

lin of GAE-treated cells (250 μg/ml) has shown no significant change when compared with control.

3.7. Alteration of cellular morphology and disruption of interphase microtubule network of A549 and HeLa cells by GAE

To investigate the effect of GAE on cellular morphology of cells, cultured A549 cells were incubated in the presence 0, 10, 25, 50, 125 and 250 μg/ml and HeLa cells were incubated in the presence of 0, 125 and 250 μg/ml of GAE for 24 h. The images of GAE-treated cells were taken by phase-contrast microscope (Fig. 5). Control (untreated) cultured cells showed normal cellular morphology (Figs. 5A for A549 cells and 5G for HeLa cells) but aberrations in the cellular morphology and shrinkage of cellular structure of GAE-treated cells were observed in a dose-dependent manner. For example, at a dose of 10 μg/ml, no change in morphology of A459 cells was observed (Fig. 5B); however, changes in the morphology of cells began at a dose of 25 μg/ml (Fig. 5C). At a dose of 50 μg/ml GAE, roundness of A549 cells was observed (Fig. 5D) and at higher doses such as 125 and 250 μg/ml, a drastic alteration of cellular morphology of A549 cells was observed (Figs. 5E and F). Significant changes in cellular morphology were observed when HeLa cells were treated with 125 and 250 μg/ml of GAE for 24 h (Fig. 5H and I).

Tubulin–microtubules system has an important role to maintain cellular morphology. Since, GAE effectively altered cellular morphology of carcinoma cells (Fig. 5), we were interested to know whether GAE targets microtubule structure in those cultured cells. These were examined by confocal microscopy using mouse monoclonal anti-α-tubulin antibody. In control A549 cells and HeLa cells, regular interphase microtubular organizations with fiber-like structures were observed (Fig. 6A and G). Treatment with GAE showed effect on microtubule network in a dose-dependent manner. At lower concentration of GAE (10 μg/ml), no significant amount of disruption of microtubules structure of A549 cells was observed (Fig. 6B). At 25 μg/ml dose of GAE, a little disruption of microtubule network of A549 cells was observed throughout the cell population. Moderate amount of disruption of A549 cellular microtubule network with shrinkage of cytoskeletal structures was observed at 50 μg/ml dose of GAE (Fig. 6D). At a higher concentration (125 μg/ml) and at IC_{50} dose significant disruption of the cellular microtubules was observed along with the loss of cellular structure (Fig. 6E and F). A similar type of disruption of cellular microtubule network was observed in HeLa cells, treated with 125 and 250 μg/ml GAE (Fig. 6H and I), respectively.

3.8. Inhibition of temperature-dependent reassembly of cold-treated depolymerized microtubule of A549 and HeLa cells by GAE

The polymerization of tubulin into microtubule is a temperature-dependent reversible process. At cold condition (4 °C), the microtubule is depolymerized into tubulin dimer and the reassembly of tubulin into microtubules occurs at 37 °C. We were interested to know whether GAE inhibits reassembly of the cold depolymerized tubulin into microtubules in the cancer cells. We observed that reassembly of the cold depolymerized interphase microtubules of A549 and HeLa cells was inhibited by GAE in a concentration-dependent manner. Cold treatment (4 °C) of A549 and HeLa cells for 5 h caused depolymerization as well as shortening of cellular interphase microtubules (Fig. 7A and E). After the cold treatment, cold media were replaced with warm media (37 °C) containing different doses of GAE (0, 125 and 250 μg/ml), incubated at 37 °C in CO_2 incubator for 2 h and images were taken by confocal microscopy. In GAE-untreated cells, interphase microtubule structures were formed within 2 h of incubation at 37 °C in both A549 cells and HeLa cells (Fig. 7B and F), while treatment with GAE inhibited the reassembly process in both the cell lines. In the presence of 125 μg/ml GAE, few distorted interphase microtubules were formed after 2 h at 37 °C (Fig. 7C and G) and at 250 μg/ml concentration the assembly process was completely inhibited

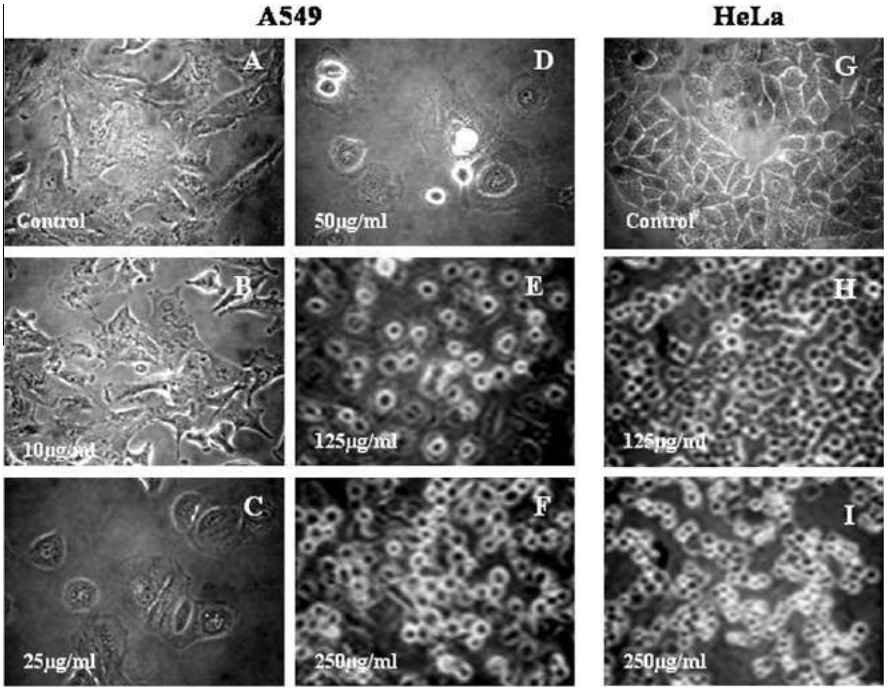

Fig. 5. Alteration of cellular morphology of carcinoma cells upon GAE treatment. Phase-contrast images are showing changes in cellular morphology of A549 cells (A–F) as well as of HeLa cells (G–I). Cultured A549 cells were treated with 0, 10, 25, 50, 125 and 250 μg/ml of GAE for 24 h, and HeLa cells were treated with 0, 125 and 250 μg/ml of GAE for 24 h. (A and G) are representing control A549 and HeLa cells. (B–F) are treated A549 cells (10–250 μg/ml) and (H–I) are treated HeLa cells (125–250 μg/ml). After treatment Phase-contrast pictures were taken using Olympus inverted microscope model CKX41.

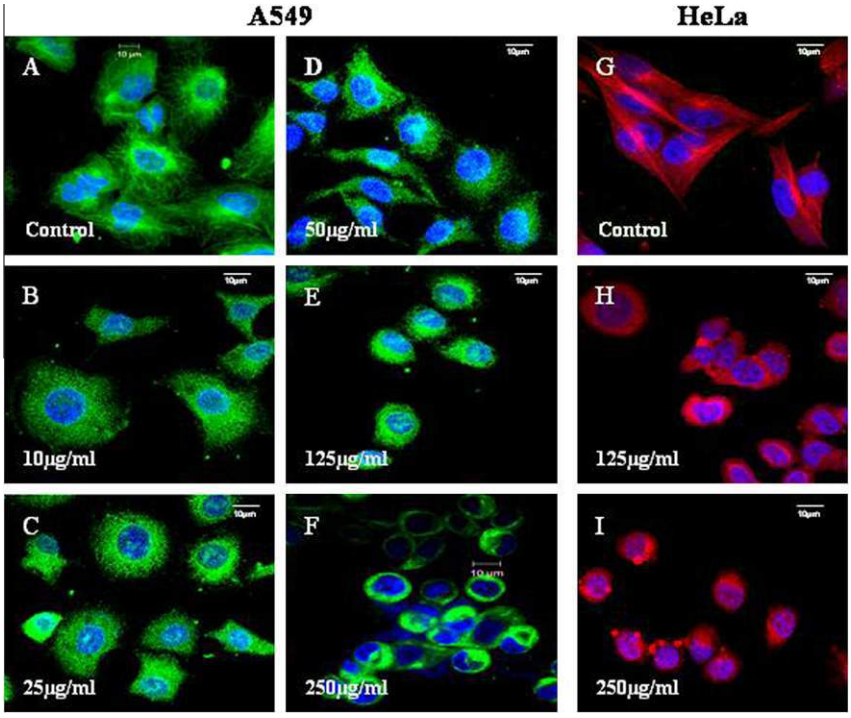

Fig. 6. Alteration of interphase microtubular structures of cancer cells upon GAE treatment. Panels (A–F) and (G–I) are representing immunofluorescence studies of interphase microtubules disruption of A549 and HeLa cells, respectively, after GAE treatment. Cultured A549 cells were treated with 0 (A), 10 (B), 25 (C), 50 (D), 125 (E) and 250 μg/ml (F) of GAE for 24 h. Cultured HeLa cells were treated with 0 (G), 125 (H) and 250 μg/ml (I) of GAE for 24 h (details of the experiments are described in Section 2). For control and treated cells, images of microtubules were taken under a confocal microscope using FITC-tagged-anti-α-tubulin antibody (green) for A549 cells, and anti-α-tubulin antibody and the corresponding rhodamine-conjugated secondary antibody (red) for HeLa cells. Nucleus was stained with DAPI (blue).

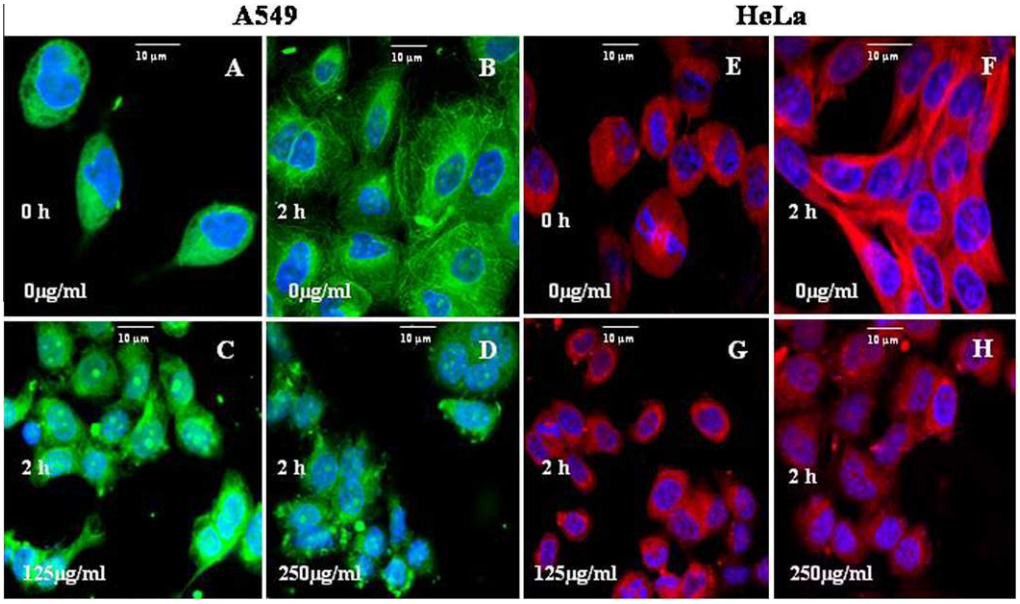

Fig. 7. Immunofluorescence study of tubulin reassembly in A549 and HeLa cells in the presence of GAE after cold depolymerization. Microtubules of A549 and HeLa cells were depolymerized by incubation at 4 °C for 5 h (A and E). Cold media were replaced by warm media containing 0 (B and F), 125 (C and G) and 250 μg/ml GAE (D and H) of GAE and incubated at 37 °C for 2 h. For A549 cells, microtubule is tagged by FITC (green) and for HeLa cells, microtubule is tagged with rhodamine (red) and both cell lines' nuclei are stained with DAPI (blue). Details of the experiment are given in Section 2.

(Fig. 7D and H). These results clearly support that GAE suppressed the reassembly of interphase microtubule in cells.

3.9. Inhibition of tubulin polymerization in vitro by GAE

Since GAE was found to affect the cellular architecture of human non-small cell lung cancer (A549) cells and human epithelial carcinoma (HeLa) cells by perturbing intercellular microtubular network, we were interested to examine whether GAE directly interacts purified mammalian tubulin. One of the most important properties of tubulin is the ability of polymerization to form dynamic structure called microtubule, a very important cellular process. Inhibition of microtubule assembly by GAE was studied *in vitro* by light scattering experiment. Tubulin (10 μM) was poly-

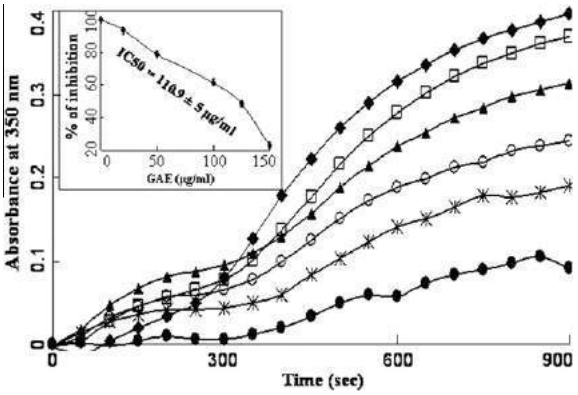

Fig. 8. *In vitro* study of inhibition of polymerization of purified tubulin by GAE. Effect of GAE on tubulin polymerization kinetics was observed by monitoring the increase in light scattering at 350. Tubulin was polymerized in the presence of 0 (-●-), 20 (-○-), 50 (-▲-), 100 (-x-), 125 (-ж-) and 150 μg/ml (-Δ-) GAE at 37 °C. (Inset) A plot of % of inhibition of tubulin polymerization against concentrations of GAE. Data represent mean ± SD of three similar experiments.

merized in the absence or presence of different doses (0–150 μg/ml) of GAE. The GAE was found to inhibit the rate and extent of tubulin polymerization in a dose-dependent manner (Fig. 8). The percentage inhibition of microtubule polymerization was calculated using the steady-state absorbance readings (at 350 nm) in the absence and presence of different doses of GAE. Fifty percent inhibition of microtubule polymerization (IC_{50}) occurred at GAE dose of 110.9 ± 5 μg/ml, while GAE dose as high as 150 μg/ml resulted in ~78 ± 2% inhibition of tubulin polymerization. Inset of Fig. 8 represents a plot of percent of polymerization inhibition upon GAE treatment.

4. Discussion

Since long ago, people all over the world have been using herbs for therapeutic purposes. In India (described in the Atharva Veda) herbs are being used as traditional medicine from 1500 BC, and in China the use of herbs for therapeutics is as old as ~2700 BC (described in Neijing Sawen). In present days, almost 90% of rural population depends on herbal medicines in the developing countries (Osunderu, 2009). Use of herbs in therapeutics becomes very popular and counts a trade of US$ 85 billion annually world wide. Now a days there are a number of natural products developed for anticancer therapy. Some of them are in different phases of clinical trial (Jordan and Wilson, 2004; Acharya et al., 2008, 2009; Panda et al., 1998; Gupta et al., 2006; Pendleton et al., 2008). Again, in some cases herbal extracts are showing more potency than the purified components (Seeram et al., 2004, 2005).

In this work, we have demonstrated the anti-cancer effect of aqueous extract of ginger (GAE) through its interaction with tubulin and microtubule equilibrium in cells. According to our study the aqueous ginger extract induces apoptosis of cancer cells, and the IC_{50} doses are 239.4 + 7.4 and 253.4 ± 8.9 μg/ml for A549 and HeLa cell lines, respectively (Fig. 1). We also demonstrated that GAE induces cellular apoptosis (Fig. 3) and disrupts cellular interphase microtubules (Fig. 6), which result in the alteration of cellular morphology (Fig. 5). GAE also inhibits the temperature-dependent reassembly of cellular microtubules (Fig. 7). Interaction of GAE with tubulin was further confirmed by *in vitro* study. We found that GAE inhibits tissue-purified tubulin polymerization, a very important functional property of tubulin, with an IC_{50} value of 110.9 ± 5.0 μg/ml (Fig. 8).

GAE inhibits microtubule structure and functions, and treatment of GAE results in the increase in cell population in $SubG_0/G_1$ phase for both A549 and HeLa cells (Fig. 2). The p53 plays an important role for controlling cellular apoptosis via different pathways. So we were interested to look for mitochondrial membrane integrity and we found loss of mitochondrial membrane potential of A549 cells upon GAE incubation (Fig. 4A). The loss of mitochondrial membrane potential leads to increase in Bax/Bcl-2 ratio and that leads to activation of mitochondrial death cascade. To support the hypothesis we did Western blotting analysis for Bax and Bcl-2 proteins from GAE-treated A549 cells. We found that the amount of pro-apoptotic protein Bax has increased along with a decrease of anti-apoptotic protein Bcl-2 in GAE-treated A549 cells (Fig. 4B). The common terminal mediator of mitochondrial death cascade is activation of caspase3. Active caspase3 generates via proteolytic cleavage of pro-caspase3. So the decrease in pro-caspase3 level indirectly indicates the increase in active caspase3 level. We found a good amount of degradation of pro-caspase3 level in A549 cells at IC_{50} dose (Fig. 4B). Although many of these microtubule targetting agents were reported to active the G_2/M check point and block the cell cycle progression, however, there are considerable evidences that show damage of microtubule structure can activate G_1 check point also (Blajeski et al., 2002; Kisurina-Evgen′eva et al., 2006; Sablima et al., 2001). It was reported that after the cell receives a pro-apoptotic signal, p53 can be transferred into mitochondria, interact with Bcl-2 protein, and change the outer membrane permeability (Moll et al., 2005). It was also determined that treatment of taxol and nocodazole to MCF-7 cells activates p53, which increases the expression of pro-apoptotic protein Bax (Kisurina-Evgen′eva et al., 2006). Although immense works are going on to understand the detailed mechanism of apoptosis by microtubule disrupting agent. it is remaining unclear. The mechanism of microtubule targeting agents inducing apoptosis is more complicated and more diverse (Blajeski et al., 2002).

Now the question may be arisen whether GAE-induced cell death causes the changes in morphology and microtubule structure of cells or disruption of microtubule by GAE causes apoptosis and loss of cell viability. To address this question we examined the effect of GAE at lower concentrations (10–50 μg/ml) on cell viability, apoptosis, inhibition of DNA synthesis, and changes in morphology and microtubules structure of A549 cells. We found, that at these concentrations of GAE, no significant amount of loss of cell viability (Fig. 1A), increase of population in $subG_0/G_1$ phase of cell cycle (Fig. 2), apoptosis (Fig. 3), and inhibition of DNA synthesis (Supplementary Fig. 1) were occurred. However, significant disruption of microtubules structure (Fig. 6B–D) and accompanied by changes in morphology of A549 cells (Fig. 5B–D) were observed at these lower doses of GAE. These results clearly indicate that damage of microtubules structure is the early event of GAE-induced cytotoxicity of cancer cells. Further purification of active component(s) from GAE and evaluation of potentiality of a single or a combination of components is necessary for the development of potential chemotherapeutic agent.

Conflict of Interest

The authors declare that there are no conflicts of interest.

Acknowledgments

The work was supported by grant from BRNS/DAE, Govt. of India (No. 2006/37/21/BRNS) to G.C. Confocal Microscope and FACS facilities are developed by the grant from National Common Minimum Program, Govt. of India. D.C. is supported by a fellowship from BRNS/DAE grant and A.D. is supported by a fellowship from Calcutta University.

Appendix A. Supplementary data

Supplementary data associated with this article can be found, in the online version, at doi:10.1016/j.fct.2010.07.020.

References

Acharya, B.R., Bhattacharyya, B., Chakrabarti, G., 2008. The natural naphthoquinone plumbagin exhibits antiproliferative activity and disrupts the microtubule network through tubulin binding. Biochemistry 47, 7838–7845.

Acharya, B.R., Choudhury, D., Das, A., Chakrabarti, G., 2009. Vitamin K3 disrupts the microtubule networks by tubulin binding: a novel mechanism of its anti proliferative activity. Biochemistry 48, 6963–6974.

Blajeski, A.P., Phan, V.A., Kottke, T.J., Kaufmann, H., 2002. G1 and G2 cell-cycle arrest following microtubule depolymerization in human breast cancer cells. J. Clin. Invest. 110, 91–99.

Bradford, M.M., 1976. A rapid and sensitive method for the quantitation of microgram quantities of protein utilizing the principle of protein–dye binding. Anal. Biochem. 72, 248–254.

Das, A., Bhattacharya, A., Chakrabarti, G., 2009. Cigarette smoke extract induces disruption of structure and function of tubulin-microtubule in lung epithelium cells and in vitro. Chem. Res. Toxicol. 22, 446–459.

Downing, K.H., 2000. Structural basis for the interaction of tubulin with proteins and drugs that affects microtubule dynamics. Annu. Rev. Cell. Dev. Biol. 16, 89–111.

Gaskin, F., Cantor, C.R., Shelanski, M.L., 1974. Turbidimetric studies of the in vitro assembly and disassembly of porcine neurotubules. J. Mol. Biol. 89, 737–755.

Gupta, K.K., Bharne, S.S., Rathinasamy, K., Naik, N.R., Panda, D., 2006. Dietary antioxidant curcumin inhibits microtubule assembly through tubulin binding. FEBS J. 273, 5320–5332.

Hamel, E., Lin, C.M., 1981. Glutamate-induced polymerization of tubulin: characteristics of the reaction and application to the large-scale purification of tubulin. Arch. Biochem. Biophys. 209, 29–40.

Jordan, M.A., Wilson, L., 2004. Microtubules as a target for anticancer drugs. Nat. Rev. Cancer 4, 253–265.

Kato, A., Higuchi, Y., Goto, H., Kizu, H., Okamoto, T., Asano, N., Hollinshead, J., Nash, R.J., Adachi, I., 2006. Inhibitory effects of *Zingiber officinale* roscoe derived components on aldose reductase activity in vitro and in vivo. J. Agric. Food Chem. 54, 6640–6644.

Khan, N., Afaq, F., Mukhtar, H., 2007. Apoptosis by dietary factors: the suicide solution for delaying cancer growth. Carcinogenesis 28, 233–239.

Kisurina-Evgen′eva, O.P., Bryantseva, S.A., Shtil, A.A., Onishchenko, G.E., 2006. Antitubulin agents can initiate different apoptotic pathways. Cell Biophys. 51, 771–775.

Lee, S.M., Cekanova, M., Back, S.J., 2007. Multiple mechanisms are involved in 6-Gingerol induced cell growth arrest and apoptosis in human colorectal cancer cells. Mol. Carcinogen. 47 (3), 197–208.

Leoni, L.M., Hamel, E., Genini, D., Shih, H., Carrera, C.J., Cottam, H.B., Carson, D.A., 2000. Indanocine, a microtubule binding indanone and a selective inducer of apoptosis in multidrug resistance cancer cells. J. Natl. Cancer Inst. 92, 224–271.

Lodish, H., Berk, A., Zipursky, S.L., Matsudaira, P., Baltimore, D., Darnell, J., 2000. Molecular Cell Biology, fourth ed. W.H. Freeman and company, New York.

Lopus, M., Panda, D., 2006. The benzophenanthridine alkaloid sanguinarine perturbs microtubule assembly dynamics through tubulin binding; a possible mechanism for its antiproliferative activity. FEBS J. 273, 2139–2150.

Moll, U.M., Wolf, S., Speidel, D., Deppert, W., 2005. Transcription-independent pro-apoptotic functions of p53. Curr. Opin. Cell Biol. 17, 631–636.

Osunderu, O.A., 2009. Sustainable Production of Traditional Medicines in Africa. Appropriate Technologies for Environmental Protection in the Developing World. Springer, Netherlands. pp. 43–51.

Panda, D., DeLuca, K., Williams, D., Jordan, M.A., Wilson, L., 1998. Antiproliferative mechanism of action of cryptophycin-52: kinetic stabilization of microtubule dynamics by high-affinity binding to microtubule ends. Proc. Natl. Acad. Sci. 95, 9313–9318.

Pendleton, J.M., Tan, W.W., Anai, S., Chang, M., Hou, W., Shiverick, K.T., Rooser, C.T., 2008. Phase II trial of isoflavone in prostate-specific antigen recurrent prostate cancer after previous local therapy. BMC Cancer 132, 1–10.

Sablima, A.A., Chumakov, P.T., Levine, A.J., Kopnin, B.P., 2001. p53 activation in response to microtubule disruption is mediated by integrin-Erk signaling. Oncogene 20, 899–909.

Saha, S., Smith, R.M., Lenz, E., Wilson, L.D., 2003. Analysis of a ginger extract by high-performance liquid chromatography coupled to nuclear magnetic resonance spectroscopy using superheated deuterium oxide as mobile phase. J. Chromatogr. 991 (1), 143–150.

Seeram, N.P., Adams, L.S., Hardy, M.L., Herber, D., 2004. Total cranberry extract versus its phytochemical constituents: antiproliferative and synergistic effects against human tumor cell lines. J. Agric. Food Chem. 52, 2512–2517.

Seeram, N.P., Adams, L.S., Henning, S.M., Nilu, Y.T., Zhang, Y.J., Nair, M.G., Heber, D., 2005. In vitro antiproliferative, apoptotic and antioxidant activities of punicalagin, ellagic acid and a total pomegranate tannin extract are enhanced in combination with other polyphenols as found in pomegranate juice. J. Nutr. Biochem. 16, 360–367.

Singleton, V.L., Orthofer, R., Lamuela-Raventó n, R.N., 1999. Analysis of total phenol and other oxidation substrates and antioxidants by means of Folin–Ciocalteu reagent. Methods Enzymol., 152–178.

White, B., 2007. Ginger: an overview. Am. Fam. Physician 75, 1689–1691.

Wu, S J., Ng, L.T., Wang, G.H., Huang, Y.J., Chen, J.L., Sun, F.M., 2009. Chlorophyll a, an active anti-proliferative compound of *Ludwigia octovalvis*, 3 activates the CD95 (APO-1/CD95) system and AMPK pathway in 3T3-L1 cells. Food Chem. Toxicol. Ahead of print.

Xin-Yi, X., Yong-Ming, W., Bao-Shan, H., Bin, Y., Lian-Jun, P., Yi-Chao, S., Bao-Fang, J., Yong, S., Ying-Xi, C., Yu-Feng, H., 2008. Evaluation of sperm mitochondrial membrane potential by JC-1 fluorescent staining and flow cytometry. Zhonghua Nan Ke Xue 14, 135–138.